

The National Direct-Drive Program: OMEGA to the National Ignition Facility

S. P. Regan, V. N. Goncharov, T. C. Sangster, E. M. Campbell, R. Betti, K. S. Anderson, T. Bernat, A. Bose, T. R. Boehly, M. J. Bonino, D. Cao, R. Chapman, T. J. B. Collins, R. S. Craxton, A. K. Davis, J. A. Delettrez, D. H. Edgell, R. Epstein, M. Farrell, C. J. Forrest, J. A. Frenje, D. H. Froula, M. Gatu Johnson, C. Gibson, V. Yu. Glebov, A. Greenwood, D. R. Harding, M. Hohenberger, S. X. Hu, H. Huang, J. Hund, I. V. Igumenshchev, D. W. Jacobs-Perkins, R. T. Janezic, M. Karasik, R. L. Keck, J. H. Kelly, T. J. Kessler, J. P. Knauer, T. Z. Kosc, S. J. Loucks, J. A. Marozas, F. J. Marshall, R. L. McCrory, P. W. McKenty, D. D. Meyerhofer, D. T. Michel, J. F. Myatt, S. P. Obenschain, R. D. Petrasso, N. Petta, P. B. Radha, M. J. Rosenberg, A. J. Schmitt, M. J. Schmitt, M. Schoff, W. Seka, W. T. Shmayda, M. J. Shoup III, A. Shvydky, A. A. Solodov, C. Stoeckl, W. Sweet, C. Taylor, R. Taylor, W. Theobald, J. Ulreich, M. D. Wittman, K. M. Woo & J. D. Zuegel

To cite this article: S. P. Regan, V. N. Goncharov, T. C. Sangster, E. M. Campbell, R. Betti, K. S. Anderson, T. Bernat, A. Bose, T. R. Boehly, M. J. Bonino, D. Cao, R. Chapman, T. J. B. Collins, R. S. Craxton, A. K. Davis, J. A. Delettrez, D. H. Edgell, R. Epstein, M. Farrell, C. J. Forrest, J. A. Frenje, D. H. Froula, M. Gatu Johnson, C. Gibson, V. Yu. Glebov, A. Greenwood, D. R. Harding, M. Hohenberger, S. X. Hu, H. Huang, J. Hund, I. V. Igumenshchev, D. W. Jacobs-Perkins, R. T. Janezic, M. Karasik, R. L. Keck, J. H. Kelly, T. J. Kessler, J. P. Knauer, T. Z. Kosc, S. J. Loucks, J. A. Marozas, F. J. Marshall, R. L. McCrory, P. W. McKenty, D. D. Meyerhofer, D. T. Michel, J. F. Myatt, S. P. Obenschain, R. D. Petrasso, N. Petta, P. B. Radha, M. J. Rosenberg, A. J. Schmitt, M. J. Schmitt, M. Schoff, W. Seka, W. T. Shmayda, M. J. Shoup III, A. Shvydky, A. A. Solodov, C. Stoeckl, W. Sweet, C. Taylor, R. Taylor, W. Theobald, J. Ulreich, M. D. Wittman, K. M. Woo & J. D. Zuegel (2018) The National Direct-Drive Program: OMEGA to the National Ignition Facility, *Fusion Science and Technology*, 73:2, 89-97, DOI: [10.1080/15361055.2017.1397487](https://doi.org/10.1080/15361055.2017.1397487)

To link to this article: <https://doi.org/10.1080/15361055.2017.1397487>



Published online: 28 Dec 2017.



Submit your article to this journal [↗](#)



Article views: 128



View related articles [↗](#)



View Crossmark data 



The National Direct-Drive Program: OMEGA to the National Ignition Facility

S. P. Regan,^{a*} V. N. Goncharov,^a T. C. Sangster,^a E. M. Campbell,^a R. Betti,^a K. S. Anderson,^a T. Bernat,^b A. Bose,^a T. R. Boehly,^a M. J. Bonino,^a D. Cao,^a R. Chapman,^a T. J. B. Collins,^a R. S. Craxton,^a A. K. Davis,^a J. A. Delettrez,^a D. H. Edgell,^a R. Epstein,^a M. Farrell,^c C. J. Forrest,^a J. A. Frenje,^d D. H. Froula,^a M. Gatu Johnson,^d C. Gibson,^c V. Yu. Glebov,^a A. Greenwood,^c D. R. Harding,^a M. Hohenberger,^c S. X. Hu,^a H. Huang,^c J. Hund,^b I. V. Igumenshchev,^a D. W. Jacobs-Perkins,^a R. T. Janezic,^a M. Karasik,^f R. L. Keck,^a J. H. Kelly,^a T. J. Kessler,^a J. P. Knauer,^a T. Z. Kosc,^a S. J. Loucks,^a J. A. Marozas,^a F. J. Marshall,^a R. L. McCrory,^{a*} P. W. McKenty,^a D. D. Meyerhofer,^g D. T. Michel,^a J. F. Myatt,^a S. P. Obenshain,^f R. D. Petrasso,^d N. Petta,^b P. B. Radha,^a M. J. Rosenberg,^a A. J. Schmitt,^f M. J. Schmitt,^g M. Schoff,^c W. Seka,^a W. T. Shmayda,^a M. J. Shoup III,^a A. Shvydky,^a A. A. Solodov,^a C. Stoeckl,^a W. Sweet,^c C. Taylor,^a R. Taylor,^a W. Theobald,^a J. Ulreich,^a M. D. Wittman,^a K. M. Woo,^a and J. D. Zuegel^a

^aUniversity of Rochester, Laboratory for Laser Energetics, Rochester, New York

^bSchafer Corporation, Livermore, California

^cGeneral Atomics, San Diego, California

^dMassachusetts Institute of Technology, Plasma Science and Fusion Center, Cambridge, Massachusetts

^eLawrence Livermore National Laboratory, Livermore, California

^fNaval Research Laboratory, Washington, District of Columbia

^gLos Alamos National Laboratory, Los Alamos, New Mexico

Received August 8, 2017

Accepted for Publication October 16, 2017

Abstract — *The goal of the National Direct-Drive Program is to demonstrate and understand the physics of laser direct drive (LDD). Efforts are underway on OMEGA for the 100-Gbar Campaign to demonstrate and understand the physics for hot-spot conditions and formation relevant for ignition at the 1-MJ scale, and on the National Ignition Facility to develop an understanding of the direct-drive physics at long scale lengths for the MJ Direct-Drive Campaign. The strategy of the National Direct-Drive Program is described; the requirements for the deuterium-tritium cryogenic fill-tube target being developed for OMEGA are presented; and preliminary LDD implosion measurements of hydrodynamic mixing seeded by laser imprint, the target-mounting stalk, and microscopic surface debris are reported.*

Keywords — *Direct-drive inertial confinement fusion, 100-Gbar Campaign.*

Note — *Some figures may be in color only in the electronic version.*

I. INTRODUCTION

The goal of the National Direct-Drive Program is to demonstrate and understand the physics of laser direct

drive^{1–3} (LDD). The program is based on the 100-Gbar Campaign on the 60-beam, 30-kJ, 351-nm OMEGA laser⁴ and the Megajoule Direct-Drive (MJDD) Campaign at the 192-beam, 1.8-MJ, 351-nm National Ignition Facility⁵ (NIF). The 100-Gbar Campaign on OMEGA explores the formation of hot-spot conditions

*E-mail: sreg@lle.rochester.edu

relevant for ignition at the 1-MJ scale. OMEGA deuterium-tritium (DT) cryogenic implosions are hydrodynamically scaled from NIF ignition designs.^{1,3} The hot-spot pressure P_{hs} is an invariant metric with respect to laser energy; consequently, achieving 100 Gbar on OMEGA ensures that 100 Gbar would be achieved on the NIF assuming similar energy coupling at the two target scales. Current DT cryogenic implosions on OMEGA achieve a $P_{\text{hs}} = 56 \pm 7$ Gbar, which is nearly half of the ignition-threshold pressure $P_{\text{hs}} = 120$ to 150 Gbar for direct-drive inertial confinement fusion (ICF) scaled to NIF energies.⁶ The 100-Gbar Campaign involves improvements to OMEGA, improvements to the targets, enhancements in diagnostics, and new modeling and simulation capabilities. In particular, it requires the development of a DT cryogenic fill-tube target having stringent tolerances for physical dimensions, material composition, surface roughness, and cleanliness.⁷ The MJDD Campaign on the NIF investigates direct-drive physics at long density scale lengths and high temperatures characteristic of coronal plasmas of direct-drive ignition targets.^{8,9} Currently only polar-direct-drive¹⁰ implosions can be performed on the NIF with the current beam configuration^{8–10}; however, spherical direct drive is the ultimate goal of the National Direct-Drive Program. A reconfiguration study is underway to convert the NIF from the current polar arrangement of laser beams around the target chamber to a spherical distribution. The National Direct-Drive Program aims to demonstrate that direct-drive ignition-scale coronal plasmas meet the laser-plasma interactions (LPIs), energy coupling, and laser-imprint requirements on the NIF and to demonstrate 100 Gbar on OMEGA in the early part of the 2020 decade. The first fill-tube DT cryogenic implosion on OMEGA is expected in 2020 (Ref. 7).

This paper concentrates on the 100-Gbar Campaign on OMEGA and the development of the fill-tube DT cryogenic target. Section II highlights the ignition threshold pressure and the generalized Lawson criterion without alpha heating. Section III describes the research areas of the 100-Gbar Campaign and presents the target specifications for the fill-tube DT cryogenic target based on hydrodynamic simulations. Section IV describes initial target physics experiments that examine these specifications. Section V presents our concluding remarks.

II. LASER DIRECT DRIVE

The P_{hs} and conversion efficiency of the laser energy into shell kinetic energy and hot-spot thermal energy

E_{hs} are critical parameters for ignition. The hot-spot pressure scales¹ as

$$P_{\text{hs}} \sim P_{\text{abl}}^{1/3} v_{\text{imp}}^{10/3} / \alpha,$$

where

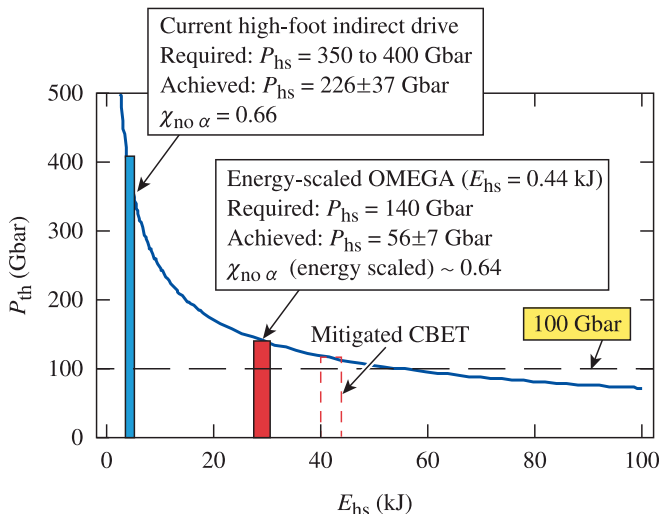
P_{abl} = ablation pressure

v_{imp} = implosion velocity (maximum mass-averaged shell velocity)

α = adiabat, defined as the mass-averaged ratio of the fuel pressure to the Fermi-degenerate pressure P_{Fermi} in the dense imploding DT shell $\alpha \equiv P/P_{\text{Fermi}}$.

In the cross-beam energy transfer (CBET) process,^{11–13} nonabsorbed light that is reflected/scattered from its critical surface or refracted from the underdense plasma acts as an electromagnetic seed for the stimulated Brillouin scattering of incoming (incident) light.¹⁴ For irradiation conditions appropriate for ignition capsule designs, CBET has been shown to reduce the capsule absorption and resulting P_{abl} in OMEGA direct-drive implosions by as much as 40% (Refs. 11, 12, and 13) and simulations indicate that a reduction in P_{abl} as large as 60% could occur in NIF-scale implosions.⁹ In addition to CBET, hydrodynamic instabilities and low-mode drive asymmetries can reduce P_{hs} and generate a mix of cold fuel/ablator into the hot spot, impacting the implosion performance rate.¹⁵ Also, suprathermal electron generation by the two-plasmon-decay (TPD) instability and stimulated Raman scattering^{16, 17} (SRS), which can preheat the DT fuel, can raise α , and can lower the hot-spot pressure for a given P_{abl} and v_{imp} . However, experiments and modeling indicate that suprathermal electrons from TPD in OMEGA implosions can at the utmost reduce areal densities in moderate-adiabat implosions ($\alpha \sim 4$) by 10% and are not considered to be the dominant mechanism for the reduction in performance. SRS is not observed on OMEGA for the typical cryogenic implosions.

The ignition threshold pressure is plotted as a function of the hot-spot thermal energy $P_{\text{hs}} > 250 \text{ Gbar} / \sqrt{E_{\text{hs}}/10 \text{ kJ}}$ in Fig. 1 (Ref. 18). Increasing laser coupling and E_{hs} reduces P_{hs} required for ignition. Symmetric direct-drive-ignition capsule designs on the NIF are predicted to couple up to 40 kJ to the hot spot, resulting in a required pressure of $P_{\text{hs}} = 120$ Gbar, as shown in Fig. 1, which could be achieved in an implosion with a convergence ratio (CR) of 22 and



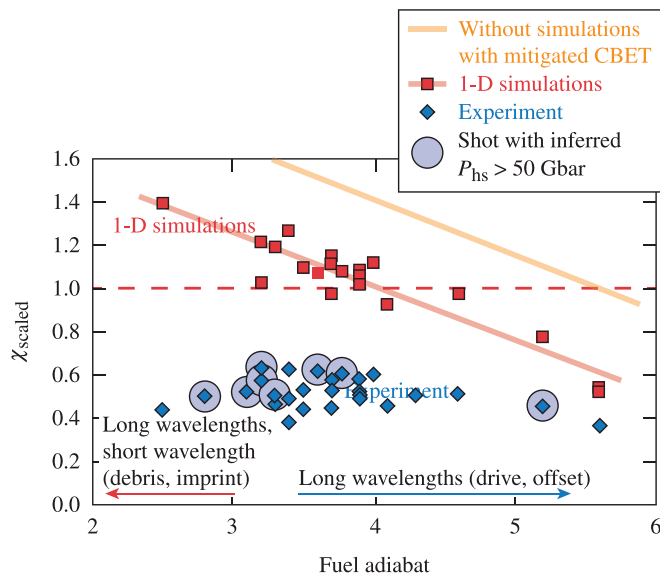
TC12311J1

Fig. 1. The ignition threshold pressure P_{th} as a function of the hot-spot energy E_{hs} . LDD and LID implosion performances are highlighted. LDD requires a hot-spot pressure above 120 Gbar to achieve ignition. CBET reduces the efficiency of coupling the laser energy to the hot spot and decreases the predicted E_{hs} from 40 to 30 kJ (corresponding to the energy-scaled OMEGA implosion achieving $E_{hs} = 0.44$ kJ without CBET mitigation) and raises P_{th} to 144 Gbar. The energy-scaled generalized Lawson criterion without alpha heating for the OMEGA direct-drive DT cryogenic implosions $\chi_{no\alpha}$ (energy scaled) is similar to the generalized Lawson criterion without alpha heating $\chi_{no\alpha}$ achieved with current indirect-drive implosions at the NIF.

an in-flight aspect ratio (IFAR)—defined as the shell radius divided by its thickness at maximum implosion velocity—of 24 if the energy coupling losses from CBET have been mitigated. Current OMEGA implosions⁶ reach $E_{hs} = 0.44$ kJ without any CBET mitigation. When scaled to 1.8 MJ of ultraviolet energy on the NIF with scaled CBET losses, these OMEGA implosions are predicted to reach $E_{hs} \approx 30$ kJ, increasing the required P_{hs} to 144 Gbar (see Fig. 1). With this E_{hs} , capsule designs with CR = 25 and an IFAR of 33 are required to reach the ignition conditions albeit with decreased robustness to hydrodynamic instabilities and low-mode drive asymmetries. Because of the required E_{hs} for direct-drive ICF, the ignition-relevant P_{hs} and CR are lower than the requirements for laser indirect-drive (LID) ICF: $P_{hs} = 350$ to 400 Gbar and CR = 30 to 40 (Ref. 19). An inferred P_{hs} of 226 ± 37 Gbar has been reported for NIF indirect-drive ICF implosions,²⁰ demonstrating that it is possible to compress DT to a pressure that exceeds the requirements for direct-drive ignition.

The highest hot-spot pressure achieved with direct-drive ICF cryogenic, layered DT implosions on OMEGA

is $P_{hs} = 56 \pm 7$ Gbar (Ref. 6). The implosion had a calculated adiabat of 3.2. This is nearly half of the ignition-threshold pressure of 120 to 150 Gbar for direct-drive ICF scaled to NIF energies. Three-dimensional (3-D) simulations suggest that low-mode distortion of the hot spot seeded by laser-drive nonuniformity and capsule-positioning error reduces the neutron rate and inferred P_{hs} (Refs. 6 and 15). As discussed in the literature, a generalized Lawson criterion without alpha heating^{21, 22} was calculated for each implosion and energy scaled^{22, 23} from the OMEGA laser energy of 26 kJ to the maximum NIF laser energy of 1.9 MJ (Refs. 6 and 22). The measured compressed areal density ρR , measured neutron yield, and one-dimensional (1-D)—calculated shocked DT mass at stagnation are used to evaluate the energy-scaled, generalized Lawson criterion without alpha heating χ_{scaled} , which is plotted in Fig. 2 as a function of fuel adiabat. The blue symbols, red symbols, and orange line represent the experimental results, the 1-D simulations including CBET, and the 1-D simulations with CBET mitigated, respectively. These hydrodynamically scaled OMEGA implosions achieved a χ_{scaled} of ~60% (Refs. 6 and 22), similar to indirect drive.^{19–21} Here P_{hs} and confinement time τ are estimated without accounting for alpha heating to assess the pure hydrodynamic



E25536J1

Fig. 2. The energy-scaled, generalized Lawson criterion without alpha heating (χ_{scaled}) is plotted as a function of fuel adiabat. The diamond symbols, square symbols, and upper solid line represent the experimental results, the 1-D simulations including CBET, and the 1-D simulations with CBET mitigated, respectively. The experimental points where the inferred $P_{hs} > 50$ Gbar are highlighted as circle symbols.

performance of the implosion. The laser-plasma coupling is assumed to be the same for OMEGA and the NIF; experiments at the NIF are ongoing to assess this assumption. As the adiabat is reduced from $\alpha = 6$, the experimental points (blue symbols in Fig. 2) deviate from the 1-D simulations including CBET (red symbols in Fig. 2). This behavior is attributed to the long-wavelength perturbations caused by laser-drive nonuniformity and capsule offsets. The χ_{scaled} for the experimental points (blue symbols in Fig. 2) peaks at $\alpha \sim 3.5$ and then decreases with decreasing adiabat. This behavior is attributed to hydrodynamic instabilities seeded by short-wavelength perturbations from microscopic surface debris, engineering features from the target stalk, and laser imprint affecting the implosion performance, in addition to the long-wavelength modes. Figure 2 shows that more-robust, higher-adiabat ignition designs could be considered if CBET were mitigated and long-wavelength perturbations were reduced.

III. 100-GBAR CAMPAIGN

The 100-Gbar Campaign is underway on OMEGA to understand the physics of assembling an ignition-relevant hot spot. Laser improvements are being made to drive a more uniform implosion and to mitigate CBET. The current method of filling the DT cryogenic capsules via permeation will be extended to a fill-tube capsule to accommodate nonpermeable ablator materials used to mitigate laser imprint and laser-plasma interactions.^{1,3} The fill-tube capsules will have less microscopic surface debris and defects, and the quicker capsule fill time will lead to less radiation damage to the ablator, which will reduce the seeds for hydrodynamic instabilities. Enhancements in diagnostics with multiple lines of sight and new modeling and simulation capabilities have been initiated to understand the 3-D effects on implosion performance. Achieving 100 Gbar on OMEGA is a critical part of the National Direct-Drive Program and will require a detailed scientific understanding of direct-drive physics.

The 100-Gbar experimental campaign is divided into ten research areas, which are outlined in Table I. Laser power balance experiments are conducted quarterly on OMEGA to understand and minimize the laser-drive nonuniformity. The target quality is being improved with the development of the fill-tube target. Laser upgrades for CBET mitigation using spatial and spectral techniques are under active investigation. Simulations—both two-dimensional (2-D) and 3-D—including CBET and hot-

TABLE I

Research Areas of the 100-Gbar Campaign

Research Area	Objective
Laser power balance	Minimize the laser-drive nonuniformity
Fill-tube target	Improve target quality (fill-tube target with polystyrene shells and multilayer ablators)
Laser upgrades for CBET mitigation	Understand and minimize coupling losses resulting from CBET (wavelength detuning, R75)
Implosion modeling/simulation	2-D and 3-D simulations including CBET and hot-electron production
1-D implosion physics and experiments	Continue to improve understanding of direct-drive physics
Laser-plasma interactions	Fundamental understanding of laser-plasma interaction (61st beam on OMEGA)
Shock timing	Measurement/modeling of shock timing
Diagnostics	Develop diagnostics to meet 100-Gbar Campaign requirements
Laser imprint	Understand and minimize effects of laser imprint
Microphysics/high-energy-density physics	Understand the microphysics relevant to LDD

electron production are being developed and routinely run for DT cryogenic implosions on OMEGA. A 1-D Implosion Physics and Experiments Campaign is being conducted to (1) investigate 1-D trends in the measured performance and (2) determine if the measured performance reaches the 1-D predictions for the limiting case of a high-adiabat implosion having a low level of multi-dimensional effects. A fundamental understanding of CBET will be explored in multibeam experiments with the tunable OMEGA P9 beam or the 61st beam of OMEGA under construction on OMEGA. Fuel preheat caused by suprathermal electrons generated by TPD is examined in OMEGA implosion experiments. Shock timing is measured and modeled for each laser pulse shape used to drive DT cryogenic implosions on OMEGA (Ref. 24). Diagnostics are developed to meet the 100-Gbar Campaign requirements. An understanding of laser imprint is being developed with the goal of minimizing the effects of laser imprint on implosion

performance. Focused experiments that test the models of the microphysics in the hydrodynamics, equation of state, opacity, thermal conductivity, and stopping power are conducted to improve the fidelity of the implosion simulations.

Improvements to the OMEGA laser are required and ongoing research will refine these needs. The 100-Gbar Campaign has 80 Gbar as a first near-term goal. The approach of the 100-Gbar Campaign is to fix the laser-drive nonuniformity while developing ways to mitigate CBET. As can be seen in Table II, the laser system requirements are less demanding for 80 Gbar. To achieve 80-Gbar hot-spot pressure with a DT cryogenic implosion having a plastic ablator and an on-target, beam-to-beam power balance averaged over 100 ps of 3% root mean square (rms) is required based on hydrodynamic simulations. CBET mitigation and multilayer ablators are not required for 80 Gbar. Achieving 80 Gbar on OMEGA will be a touchstone for physics understanding and simulations. To achieve 100-Gbar hot-spot pressure, a beam-to-beam power balance averaged over 100 ps of 1% rms and the implementation of a CBET mitigation technique (spatial, spectral, or temporal) are required. The on-target, overlapped laser-intensity uniformity depends on the laser power balance and the far-field intensity distribution of each beam on target, as well as accurate target positioning. Ultraviolet and X-ray diagnostics and experiments are being developed to characterize the laser-drive nonuniformity level on target.

Improvements in targets are required and ongoing research will refine these needs. The DT cryogenic fill-tube target requirement for the 100-Gbar Campaign is based on three factors³: (1) mitigating laser-plasma interactions using nonpermeable ablator materials, (2) minimizing target debris and defects, and (3) minimizing radiation damage to the ablator. The plastic ablator will have an embedded, nonpermeable Si layer to mitigate laser-plasma interactions and possibly a Si-doped outer plastic layer to

mitigate laser imprint.^{1,3} Since the fill-tube capsules are stored exclusively in the controlled clean-room environment of the shroud until the target is imploded, the target will have drastically less microscopic surface debris and defects than the permeation-filled targets, which sample many vacuum environments before shot time. The quicker capsule fill time of the fill-tube target compared to the permeation-filled target (i.e., days versus weeks) will lead to less radiation damage to the ablator of the fill-tube target. Both of these improvements will reduce the seeds for hydrodynamic instabilities.

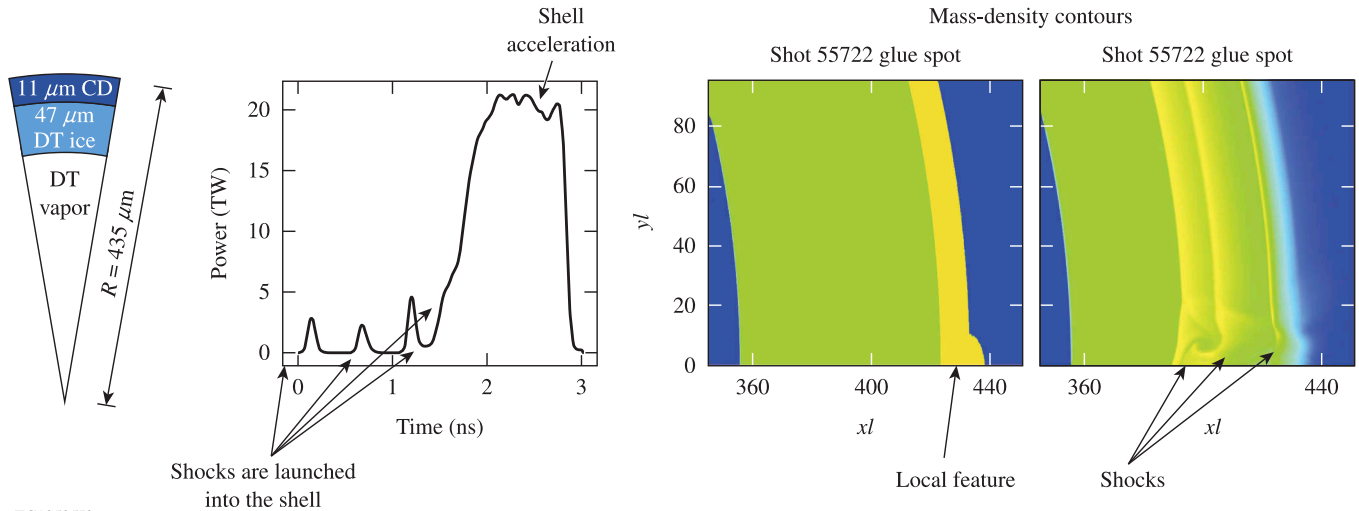
Microscopic features, including debris, domes, and depressions, on the surface of the target are considered the main seed of short-scale mix.²⁵ Characterizing cryogenic targets at the shot time is crucial for understanding target failure mechanisms. Two-dimensional implosion simulations were conducted for the target with a mass perturbation on the surface and laser pulse shown in Fig. 3. The simulated mass-density contours highlight the effects of the shock interactions with a local feature on the target surface. Simulations show that the shell mass modulation caused by the initial surface features are amplified by Richtmyer-Meshkov (RM) instability during shock transit by a factor of 3 to 5. As the shell starts to accelerate, these modulations are further amplified by the Rayleigh-Taylor (RT) instability growth. It is well known that the ablation-front RT growth is significantly reduced²⁶ by the mass-ablation effects when the amplitude modulation is small $ka < 1$, where k is the modulation wave number and a is the amplitude. In contrast, when the perturbation amplitude is large and $ka > 1$ (nonlinear regime), the mass ablation enhances the growth.²⁷ The evolution of the instability seeded by the perturbation at the target surface in the nonlinear regime is shown in Fig. 4. Each feature on the surface of the target has the potential to produce a hole in the shell, injecting ablator and cold DT into the vapor region. Injected mass as a result of instability growth should not significantly exceed the original vapor mass, which is approximately equal to 0.14 μg for OMEGA targets. Detailed target metrology analysis shows hundreds of micron-scale features on glow discharge polymer (GDP) shells, which according to simulations is more than sufficient to inject 0.14 μg of cold material into the hot spot.²⁵

The target-debris specifications shown in Table III were selected to reduce the amount of mix mass to tolerable levels. The 80-Gbar Campaign will be used as a platform to investigate the most challenging requirements of target-positioning accuracy and tolerable level

TABLE II

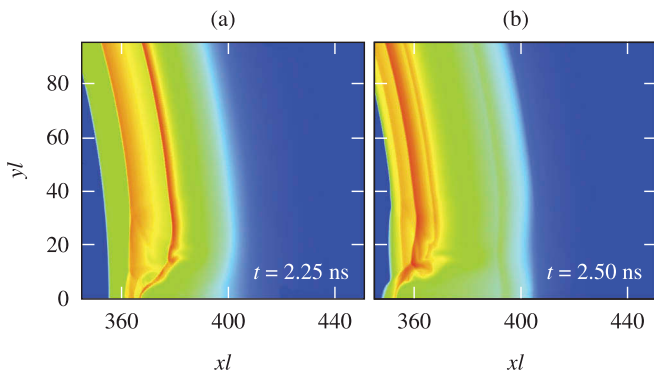
Laser Requirements for 80-Gbar and 100-Gbar Campaigns

80 Gbar	100 Gbar
1. On-target, beam-to-beam power balance integrated over 100 ps of 3% rms	1. On-target, beam-to-beam power balance integrated over 100 ps of 1% rms 2. Implementation of CBET mitigation technique (spatial, spectral, or temporal)



TC10595J2

Fig. 3. Two-dimensional simulations highlighting the effects of hydrodynamic instabilities seeded by a microscopic mass perturbation on the target surface.



E26045J1

Fig. 4. The late time evolution of the hydrodynamic instability presented in Fig. 3. The feature on the surface of the target produces a hole in the shell, injecting ablator and cold DT into the vapor region.

of microscopic features on the target surface with controlled experiments. Initial experiments will use the DT permeation-filled targets. The 80-Gbar Campaign requires a target-positioning accuracy of less than 10 μm and a tolerable amount of microscopic features and engineering features on the surface quantified as follows:

1. Count all surface defect features, including depressions, having lateral dimension d (defined as the direction parallel to the capsule surface) with $0.5 \mu\text{m} \leq d \leq 5 \mu\text{m}$ and a height h (defined as the direction perpendicular to the capsule surface) such that $h/d \geq 0.02$. Such features represent nonlinear seeds for RT growth during shell acceleration.

2. Count all surface features having $d > 5 \mu\text{m}$ and $h > 50 \text{ nm}$, including the glue securing the stalk or fill tube. These defects are amplified by linear growth of ~ 5 during the RM phase and another factor of 100 to 150 during the RT phase.

3. Each feature, as it breaks out of the shell, injects fuel and ablator mass equivalent to 4 to 5 times that of the fraction of the initial shell mass covered by the surface feature. Requiring that the total injected mass into the hot-spot region should be smaller than the initial vapor mass of $0.14 \mu\text{g}$ leads to a mix fraction f_{mix} defined as a ratio of the injected mass to the initial vapor mass, not exceeding unity. For all of the n surface features the mix fraction is calculated as $f_{mix} = \sum_{i=0}^n 10^{-3} d_{\mu\text{m}}^2$, where d is given in units of micron.

Polystyrene ablators having a superior surface smoothness to GDP shells are being explored in current experiments. Experimental results from the 80-Gbar Campaign will be used to define the target specifications for the 100-Gbar Campaign.

A conceptual design review has been completed for the fill-tube target, and a technique to characterize the surface features based on dark-field imaging has been defined. The delivery date for the fill-tube target on OMEGA is 2020.

IV. TARGET PHYSICS EXPERIMENTS

Initial target physics experiments have been conducted on OMEGA to examine the hydrodynamic mixing

TABLE III
Target Requirements for 80-Gbar and 100-Gbar Campaigns

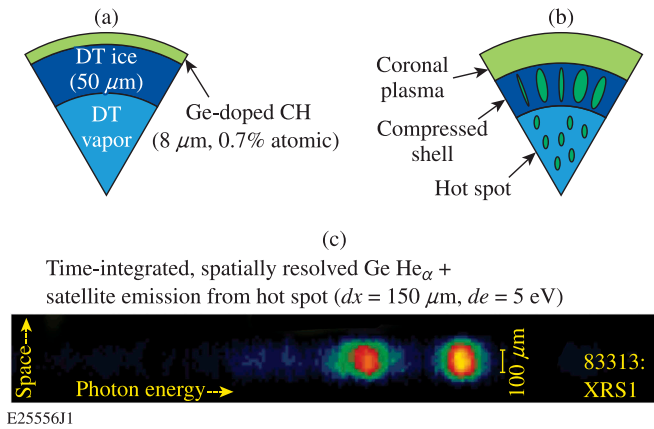
80 Gbar (Plastic Ablators)	100 Gbar (Multilayer Ablators)
<ol style="list-style-type: none"> 1. Target positioned at chamber center to <10 μm. 2. Target quality: <ol style="list-style-type: none"> a. A tolerable amount of microscopic surface features and engineering features is quantified as follows: <ol style="list-style-type: none"> (1) Count all surface defect features, including depressions, having lateral dimension d with $0.5 \mu\text{m} \leq d \leq 5 \mu\text{m}$ and a height h such that $h/d \geq 0.02$. (2) Count all surface features having $d > 5 \mu\text{m}$ and $h > 50 \text{ nm}$, including the glue securing the stalk or fill tube. (3) The mix fraction f_{mix} for all of the n surface features calculated as $f_{mix} = \sum_{i=0}^n 10^{-3} d_{\mu\text{m}}^2$, where d is given in units of micron, should not exceed unity. b. Inner surface roughness of ablator not to exceed $\sigma_{rms} = 0.5 \mu\text{m}$ in modes $\ell < 5$ and $\sigma_{rms} = 0.1 \mu\text{m}$ in modes $\ell \geq 5$. c. At cryogenic temperature, determination of the target outer diameter to <2 μm. d. At cryogenic temperature, determination of target outer surface long wavelength ($l < 10$) nonuniformity to <0.1 μm. e. DT ice layer thickness known to 0.5 μm. f. DT ice layer density known to <5%. g. Determination of the ablator atomic composition and density (C:H:O:D:T) to <10%. h. Target must be spherical with $\ell = 2$ out-of-round amplitude less than 0.7 μm. i. DT permeation-filled targets. 	<ol style="list-style-type: none"> 1. Target positioned at chamber center to <5 μm. 2. Target quality: <ol style="list-style-type: none"> a. A tolerable amount of microscopic surface features and engineering features will be based on what is learned in the 80-Gbar Campaign. <ol style="list-style-type: none"> b. Inner surface roughness of ablator same as 80 Gbar. c. Target outer diameter same as 80 Gbar. d. Target low-mode nonuniformity same as 80 Gbar. e. DT ice layer thickness same as 80 Gbar. f. DT ice layer density same as 80 Gbar. g. Determination of the ablator atomic composition and density (C:H:Si:O:D:T) to <10%. (Si layer added for TPD mitigation.) h. Same sphericity specification as 80 Gbar. i. Fill-tube capability with glue spot <30 μm to fuel multilayer ablator shells.

seeded by laser imprint, the target-mounting stalk, and microscopic surface debris. As shown in Fig. 5a, a trace amount of Ge (0.7% atomic) was added to the plastic ablator to track hydrodynamic mixing of the ablator through the DT ice layer by the ablation-front instability and into the hot-spot region as illustrated in Fig. 5b. If Ge reaches the hot spot, it will emit K-shell emission.²⁸ A time-integrated, spatially resolved X-ray spectrum of the Ge He $_{\alpha}$ and satellite emission at ~10 keV of photon energy was recorded as shown in Fig. 5c. This measurement experimentally confirms that the ablator material is mixing into the hot spot. The hot-spot mix mass inferred from the Ge He $_{\alpha}$ and satellite emission will be used to constrain the simulations and refine the target requirements, similar to target physics experiments conducted on the NIF (Refs. 29 and 30). Although this technique can detect levels of Ge-doped CH to the nanogram-level, it is

only sensitive to mass from the Ge-doped ablator. It cannot detect any DT mass that has mixed into the hot spot. In future experiments the absolute X-ray power radiated by the hot spot will be monitored and compared to the neutron yield to infer the amount of total mix mass in the hot spot,³¹⁻³³ and the effects of a fill tube on implosion performance will be investigated.

V. CONCLUSIONS

The goal of the National Direct-Drive Program is to demonstrate and understand the physics of LDD. The 100-Gbar Campaign on OMEGA and the MJDD Campaign on NIF are underway to demonstrate that direct-drive ignition-scale coronal plasmas will meet the requirements for LPIs, energy coupling, and laser imprint on the NIF and



(c) Time-integrated, spatially resolved $\text{Ge He}_\alpha +$ satellite emission from hot spot ($dx = 150 \mu\text{m}$, $de = 5 \text{ eV}$)

Fig. 5. (a) The plastic ablator is doped with a trace amount of Ge to study hydrodynamic mixing; (b) a schematic highlighting the mixing of ablator material through the DT shell and into the hot spot; and (c) the measured time-integrated and spatially resolved Ge He_α and satellite emission from the hot spot, indicating ablator material mixed into the hot spot.

will demonstrate 100 Gbar on OMEGA in the early part of the 2020 decade. The 100-Gbar Campaign involves improvements to OMEGA, improvements to the targets, enhancements in diagnostics, and new modeling and simulation capabilities. In particular, it requires the development of a DT cryogenic fill-tube target having stringent tolerances for physical dimensions, material composition, surface roughness, and cleanliness. The first fill-tube DT cryogenic implosion on OMEGA is expected in 2020. Initial target physics experiments have been conducted on OMEGA to examine the hydrodynamic mixing seeded by laser imprint, the target-mounting stalk, and microscopic surface debris.

Acknowledgments

This material is based upon work supported by the U.S. Department of Energy's (DOE's) National Nuclear Security Administration under award DE-NA0001944. Part of this work was performed under the auspices of the DOE by Lawrence Livermore National Laboratory under contract DE-AC52-07NA27344. This report was prepared as an account of work sponsored by an agency of the U.S. Government. Neither the U.S. Government nor any agency thereof, nor any of their employees, makes any warranty, express or implied, or assumes any legal liability or responsibility for the accuracy, completeness, or usefulness of any information, apparatus, product, or process disclosed, or represents that its use would not infringe privately owned rights. Reference herein to any specific commercial product, process, or service by trade name, trademark, manufacturer, or otherwise does not necessarily constitute or imply its endorsement, recommendation, or favoring by the U.S. Government or any agency thereof. The views and opinions of authors expressed

herein do not necessarily state or reflect those of the U.S. Government or any agency thereof.

References

1. V. N. GONCHAROV et al., "Improving the Hot-Spot Pressure and Demonstrating Ignition Hydrodynamic Equivalence in Cryogenic Deuterium-Tritium Implosions on OMEGA," *Phys. Plasmas*, **21**, 5, 056315 (2014); <http://dx.doi.org/10.1063/1.4876618>.
2. R. S. CRAXTON et al., "Direct-Drive Inertial Confinement Fusion: A Review," *Phys. Plasmas*, **22**, 11, 110501 (2015); <http://dx.doi.org/10.1063/1.4934714>.
3. V. N. GONCHAROV et al., "National Direct-Drive Program on OMEGA and the National Ignition Facility," *Plasma Phys. Control. Fusion*, **59**, 1, 014008 (2017); <https://doi.org/10.1088/0741-3335/59/1/014008>.
4. T. R. BOEHLI et al., "Initial Performance Results of the OMEGA Laser System," *Opt. Commun.*, **133**, 1–6, 495 (1997); [https://doi.org/10.1016/S0030-4018\(96\)00325-2](https://doi.org/10.1016/S0030-4018(96)00325-2).
5. E. M. CAMPBELL and W. J. HOGAN, "The National Ignition Facility—Applications for Inertial Fusion Energy and High-Energy-Density Science," *Plasma Phys. Control. Fusion*, **41**, 12B, B39 (1999); <https://doi.org/10.1088/0741-3335/41/12B/303>.
6. S. P. REGAN et al., "Demonstration of Fuel Hot-Spot Pressure in Excess of 50 Gbar for Direct-Drive, Layered Deuterium-Tritium Implosions on OMEGA," *Phys. Rev. Lett.*, **117**, 2, 025001 (2016); "Erratum," **117**, 5, 059903 (2016); <http://doi.org/10.1103/PhysRevLett.117.025001>.
7. D. R. HARDING et al., "Requirements and Capabilities for Fielding Cryogenic DT-Containing Fill-Tube Targets for Direct-Drive Experiments on OMEGA," *Fusion Sci. Technol.*, **73** (2018); <http://doi.org/10.1080/15361055.2017.1374812>.
8. M. HOHENBERGER et al., "Polar-Direct-Drive Experiments on the National Ignition Facility," *Phys. Plasmas*, **22**, 5, 056308 (2015); <http://dx.doi.org/10.1063/1.4920958>.
9. P. B. RADHA et al., "Direct Drive: Simulations and Results from the National Ignition Facility," *Phys. Plasmas*, **23**, 5, 056305 (2016); <http://dx.doi.org/10.1063/1.4946023>.
10. S. SKUPSKY et al., "Polar Direct Drive on the National Ignition Facility," *Phys. Plasmas*, **11**, 5, 2763 (2004); <http://dx.doi.org/10.1063/1.1689665>.
11. I. V. IGUMENSHCHEV et al., "Crossed-Beam Energy Transfer in Implosion Experiments on OMEGA," *Phys. Plasmas*, **17**, 12, 122708 (2010); <http://dx.doi.org/10.1063/1.3532817>.
12. I. V. IGUMENSHCHEV et al., "Crossed-Beam Energy Transfer in Direct-Drive Implosions," *Phys. Plasmas*, **19**, 5, 056314 (2012); <http://dx.doi.org/10.1063/1.4718594>.

13. D. H. FROULA et al., “Increasing Hydrodynamic Efficiency by Reducing Cross-Beam Energy Transfer in Direct-Drive Implosion Experiments,” *Phys. Rev. Lett.*, **108**, 12, 125003 (2012); <https://doi.org/10.1103/PhysRevLett.108.125003>.
14. C. J. RANDALL, J. R. ALBRITTON, and J. J. THOMSON, “Theory and Simulation of Stimulated Brillouin Scatter Excited by Nonabsorbed Light in Laser Fusion Systems,” *Phys. Fluids*, **24**, 8, 1474 (1981); <http://dx.doi.org/10.1063/1.863551>.
15. I. V. IGUMENSHCHEV et al., “Three-Dimensional Modeling of Direct-Drive Cryogenic Implosions on OMEGA,” *Phys. Plasmas*, **23**, 5, 052702 (2016); <http://dx.doi.org/10.1063/1.4948418>.
16. W. L. KRUER, “Frontiers in Physics,” *The Physics of Laser Plasma Interactions*, Vol. 73, D. PINES ed., Addison-Wesley, Redwood City, California (1988).
17. M. J. ROSENBERG et al., “Origins and Scaling of Hot-Electron Preheat in Ignition-Scale Direct-Drive Inertial Confinement Fusion Experiments,” *Phys. Rev. Lett.* (in print).
18. V. N. GONCHAROV et al., “Demonstrating Ignition Hydrodynamic Equivalence in Direct-Drive Cryogenic Implosions on OMEGA,” *J. Phys.: Conf. Ser.*, **717**, 012008 (2016); <https://doi.org/10.1088/1742-6596/717/1/012008>.
19. O. A. HURRICANE et al., “Fuel Gain Exceeding Unity in an Inertially Confined Fusion Implosion,” *Nature*, **506**, 7488, 343 (2014); <http://www.nature.com/nature/journal/v506/n7488/full/nature13008.html>.
20. T. DÖPPNER et al., “Demonstration of High Performance in Layered Deuterium-Tritium Capsule Implosions in Uranium Hohlräume at the National Ignition Facility,” *Phys. Rev. Lett.*, **115**, 5, 055001 (2015); <https://doi.org/10.1103/PhysRevLett.115.055001>.
21. R. BETTI et al., “Alpha Heating and Burning Plasmas in Inertial Confinement Fusion,” *Phys. Rev. Lett.*, **114**, 25, 255003 (2015); <http://dx.doi.org/10.1103/PhysRevLett.114.255003>.
22. A. BOSE et al., “Core Conditions for Alpha Heating Attained in Direct-Drive Inertial Confinement Fusion,” *Phys. Rev. E*, **94**, 1, 011201 (R) (2016); <https://doi.org/10.1103/PhysRevE.94.011201>.
23. R. NORA et al., “Theory of Hydro-Equivalent Ignition for Inertial Fusion and Its Applications to OMEGA and the National Ignition Facility,” *Phys. Plasmas*, **21**, 5, 056316 (2014); <http://dx.doi.org/10.1063/1.4875331>.
24. T. R. BOEHLI et al., “Multiple Spherically Converging Shock Waves in Liquid Deuterium,” *Phys. Plasmas*, **18**, 9, 092706 (2011); <http://dx.doi.org/10.1063/1.3640805>.
25. I. V. IGUMENSHCHEV et al., “Effects of Local Defect Growth in Direct-Drive Cryogenic Implosions on OMEGA,” *Phys. Plasmas*, **20**, 8, 082703 (2013); <http://dx.doi.org/10.1063/1.4818280>.
26. V. N. GONCHAROV et al., “Self-Consistent Stability Analysis of Ablation Fronts with Large Froude Numbers,” *Phys. Plasmas*, **3**, 4, 1402 (1996); <http://dx.doi.org/10.1063/1.871730>.
27. R. BETTI and J. SANZ, “Bubble Acceleration in the Ablative Rayleigh–Taylor Instability,” *Phys. Rev. Lett.*, **97**, 20, 205002 (2006); <http://dx.doi.org/10.1103/PhysRevLett.97.205002>.
28. B. A. HAMMEL et al., “Diagnosing and Controlling Mix in National Ignition Facility Implosion Experiments,” *Phys. Plasmas*, **18**, 5, 056310 (2011); <http://dx.doi.org/10.1063/1.3567520>.
29. S. P. REGAN et al., “Hot-Spot Mix in Ignition-Scale Implosions on the NIF,” *Phys. Plasmas*, **19**, 5, 056307 (2012); <http://dx.doi.org/10.1063/1.3694057>.
30. S. P. REGAN et al., “Hot-Spot Mix in Ignition-Scale Inertial Confinement Fusion Targets,” *Phys. Rev. Lett.*, **111**, 4, 045001 (2013); <https://doi.org/10.1103/PhysRevLett.111.045001>.
31. T. C. SANGSTER et al., “Improving Cryogenic Deuterium-Tritium Implosion Performance on OMEGA,” *Phys. Plasmas*, **20**, 5, 056317 (2013); <http://dx.doi.org/10.1063/1.4805088>.
32. T. MA et al., “Onset of Hydrodynamic Mix in High-Velocity, Highly Compressed Inertial Confinement Fusion Implosions,” *Phys. Rev. Lett.*, **111**, 8, 085004 (2013); <https://doi.org/10.1103/PhysRevLett.111.085004>.
33. R. EPSTEIN et al., “X-Ray Continuum as a Measure of Pressure and Fuel-Shell Mix in Compressed Isobaric Hydrogen Implosion Cores,” *Phys. Plasmas*, **22**, 2, 022707 (2015); <http://dx.doi.org/10.1063/1.4907667>.